SEISMIC RESISTANT WELDED CONNECTIONS FOR MRF OF CFT COLUMNS AND I BEAMS

Cristian Vulcu; Aurel Stratan; Dan Dubina
Department of Steel Structures and Structural Mechanics, "Politehnica" University of Timisoara, Romania
cristian.vulcu@ct.upt.ro; aurel.stratan@ct.upt.ro; dan.dubina@ct.upt.ro

ABSTRACT

The paper displays the experimental program aiming to characterize the behaviour of two types of moment resisting joints in multi-storey frames of concrete filled high strength RHS columns and steel beams. Moment resisting joints are of welded connection in two different typologies: with reduced beam section (RBS) and with cover plates (CP). The paper describes the design procedure of the joints and displays the specific detailing for these two solutions. Numerical simulations were realised prior to the testing in order to anticipate the behaviour of the joints and to find answers to problems for which decisions were taken in the design process. The material model used in the numerical simulations was calibrated based on the results from tensile tests. Finally, the results from the numerical analysis are presented.

1. INTRODUCTION

The design philosophy of a structure to seismic action allows for plastic deformations in dissipative members, the global stability of the structure being provided by the non-dissipative members. With the aim to investigate the seismic performance of dual frames (Vulcu *et al.* 2012), in the current research project, the beams are made of mild carbon steel (MCS) and the columns of high strength steel (HSS) (Figure 1). The investigated frames are considered to be Moment Resisting Frames (MRF), Dual Concentrically Braced Frames (D-CBF) and Dual Eccentrically Braced Fames (D-EBF).

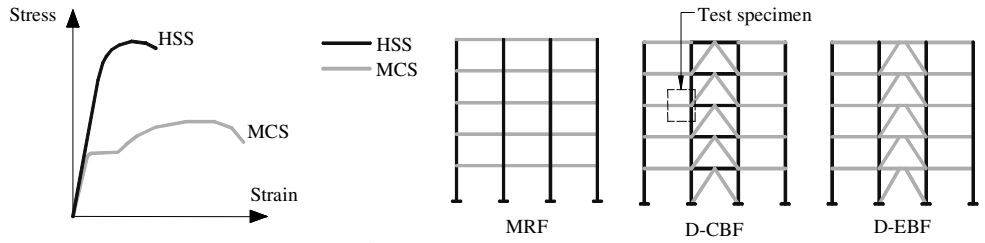

Figure 1. Frames (MRF, D-CBF, D-EBF) realized in the dual-steel concept

For the three frame typologies, the columns are realized as concrete filled high strength steel tubes. Cold formed rectangular hollow section tubes will be used for this purpose. In case of composite columns, several situations are practiced:

- The case in which the beam passes through the steel tube and transfers the load directly to the concrete core; in this case the tube has a secondary role;
- The case in which the concrete inside the tube is inactive (connectors are not positioned); it is counted on the concrete core just in case of fire;
- The case in which the concrete is active and the efforts are introduced using connectors.

In the current research program, the goal is to count on both materials (steel and concrete) and to have a composite action ensured by the use of shot fired nails. As basis for definition of the experimental program on beam-column joints, cross-sections from the D-CBF frame were used, considering two combinations of HSS/MCS:

- RHS 300x12,5 S460 column and IPE 400 S355 beam;
- RHS 250x10 S700 column and IPE 400 S355 beam.

The beams are welded to the columns considering two types of connections: with reduced beam section (RBS) (see Figure 2a), and with cover plates (CP) (see Figure 2b). Due to the flexibility of the tube walls under transverse forces, the flanges of the beam and the cover plates will not work on the entire width - which means that efforts will be transferred to the side walls of the tube by an effective width b_{eff} (see Figure 2c and Figure 2d). This is not enough to ensure a higher resistance of the connection with regard to the strength of the beam.

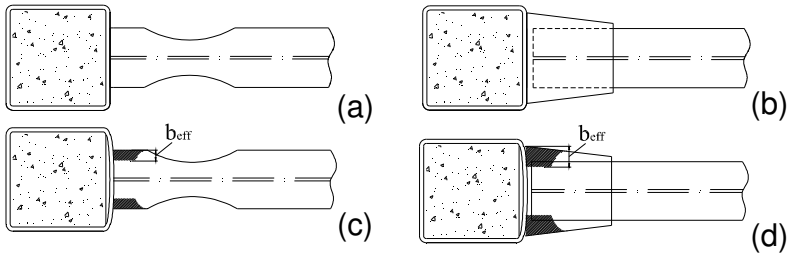

Figure 2. a) Joint with RBS, b) joint with CP, c) and d) the corresponding effective width

In the literature, different joint typologies have been studied for tubes of rectangular section as well as for tubes of circular section, see Figure 3.

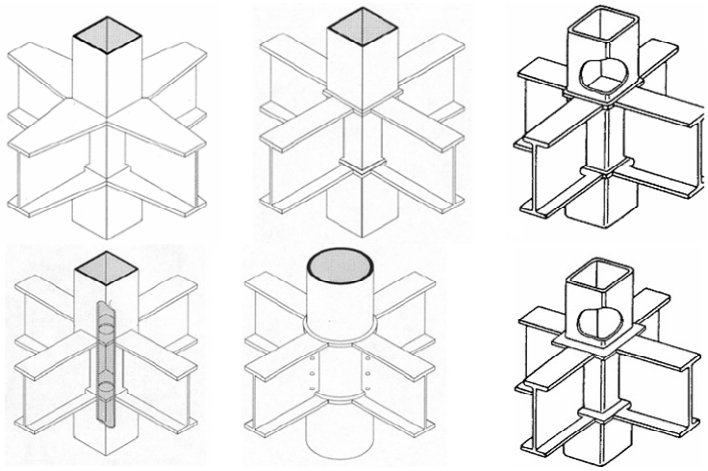

Figure 3. Existing connection solutions for welded beam-to-column joints

In order to transfer the loads uniformly to the cross section of the tube, interior diaphragms, through diaphragms as well as outer diaphragms have been used (Morino and Tsuda, 2003, and Park *et al.,* 2005). Design guidelines have been developed for these types of connections as well (Kurobane *et al.,* 2004).

2. DESIGN OF JONTS

The connection solution of the beams and columns within the current research is based on the use of stiffeners that are welded around the steel tube, and which form an outer diaphragm. From the design of the joint, the thickness of the stiffeners was higher than the thickness of the beam flanges and cover plates. Because of this, at the connection with the beam, it was proposed that a preparation of the stiffeners to be performed (see Figure 4 and Figure 5) so as to avoid the concentration of the efforts due to the variation of the thickness. This solution has the advantage that no preparations are necessary for the flanges of the beam, and respectively cover plates.

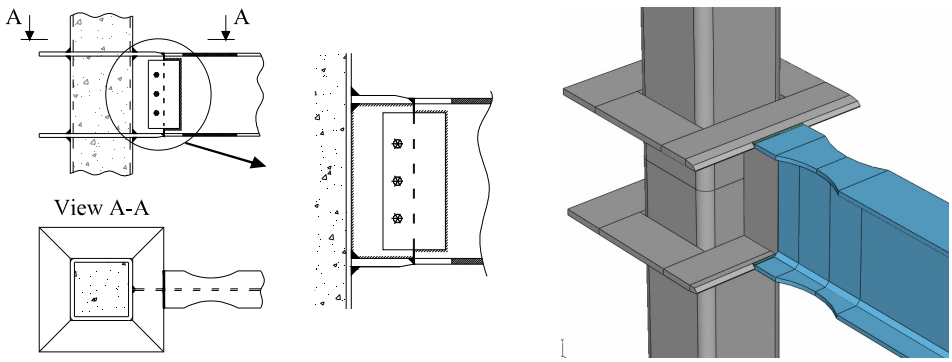

Figure 4. Joint with reduced beam section (RBS)

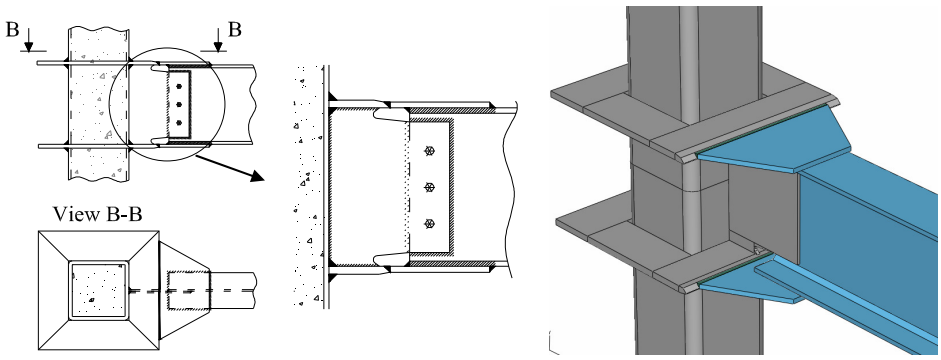

Figure 5. Joint with cover plates (CP)

Beam flanges and cover plates are welded to the column stiffeners using full-penetration butt welds. A shear tab bolted connection between the beam web and vertical column stiffener is used for erection. The final connection of the beam web is realized as full-penetration weld for the RBS joint and as fillet welds for the CP joint. The main components covered within the joint design are illustrated in Figure 6.

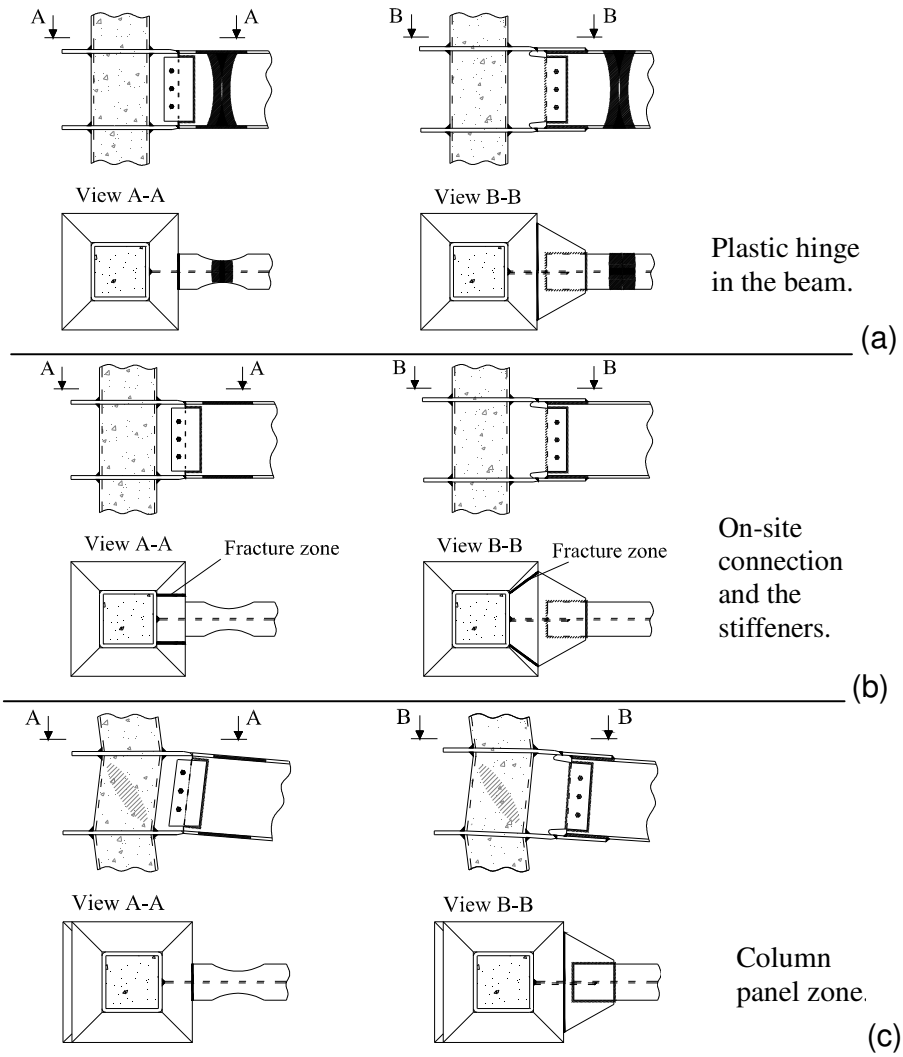

Figure 6. Main components taken into account in the design of the joints

The design of the joints was performed considering plastic hinge formation in the beams (Figure 6a). Further with bending moment and the shear force from the plastic hinge, the components of the connection were designed (welded on-site connection, stiffeners and column panel) so as to reach a higher resistance than the beam. The assumptions considered in the design of the joint components are presented further:

2.1 Plastic hinge position

The geometry of the reduced beam section was determined according to AISC 358-2005, and for the joint with cover plates it was assumed that the plastic hinge would develop at $h_{beam}/3$ from the cover plate ending based on PEER 2000/07 (Figure 6a).

2.2 Bending moment and shear force in the plastic hinge

The probable maximum moment ($M_{pl,hinge}$) and shear force ($V_{Ed,hinge}$) in the plastic hinge were determined by considering that a fully yielded and strain hardened plastic hinge develops in the beam.

$$M_{pl,hinge} = \frac{\gamma_{sh} \cdot \gamma_{ov} \cdot W_{pl} \cdot f_y}{\gamma_{M0}} \quad (1)$$

$$V_{Ed,hinge} = \frac{M_{pl,hinge}}{L'} \quad (2)$$

where γ_{sh} represents the strain hardening (γ_{sh} *=1.10*), γ_{ov} is the overstrength factor (γ_{ov}*=1.25*), f_y is the nominal yield strength of the beam, γ_{M0} is the material safety factor, W_{pl} is the plastic section modulus, and *L'* the distance between the plastic hinge and the load application point;

2.3 Welded connection between beam and cover plates

The welded connection between beam and cover plates was checked assuming that the flanges carry the moment only, while the web carries the shear force.

2.4 On-site connection

The probable maximum moment ($M_{Ed,sc}$) and shear force ($V_{Ed,sc}$) at the on-site connection were determined by considering that a fully yielded and strain hardened plastic hinge develops in the beam. As no weld access holes are used for the RBS joint, the plastic modulus of the gross cross-section of the beam was considered. The cover plates were checked assuming that the flanges carry moment only, while the web carries the shear force. It was checked that the relation $V_{Ed,sc} \le 0.5 \cdot V_{pl,Rd}$ is satisfied.

2.5 Strength of stiffeners

The probable maximum moment ($M_{Ed,cf}$) and shear force ($V_{Ed,cf}$) at the column face were determined by considering that a fully yielded and strain hardened plastic hinge forms in the beam. The force developed in the stiffeners at the connection with the beam flanges (respectively cover plates), was determined by considering that the bending moment is carried by stiffeners alone. Stiffeners were checked to fracture along the path shown in Figure 6b, neglecting the direct connection to the column wall.

2.6 Shear resistance of the column panel zone

The shear force in the column panel zone corresponds to fully-yielded plastic hinges in the beams framing into the joint. According to EN 1998-1-2004, no overstrength is required (γ_{sh}*=1.0* and γ_{ov}*=1.0*). It was assumed that the bending moments in the beam corresponds to β*=1,0*. The resistance of the column panel zone in shear (Figure 6c) was checked based on the provisions within EN 1998-1-2004 and EN 1994-1-1-2004 design codes.

3. EXPERIMENTAL PROGRAM

The objective of the experimental tests will be to pre-qualify by tests welded connections in moment resisting frames and dual braced frames designed using the dual-steel concept. Experimental tests on large specimens (see Figure 7) will be performed in order to demonstrate that joint detailing (8 configurations) and welding

technology perform adequately under seismic loading (reverse cyclic loading in the inelastic range). The main purpose is to obtain plasticization in the beam (8 specimens) and in the connection zone (8 specimens).

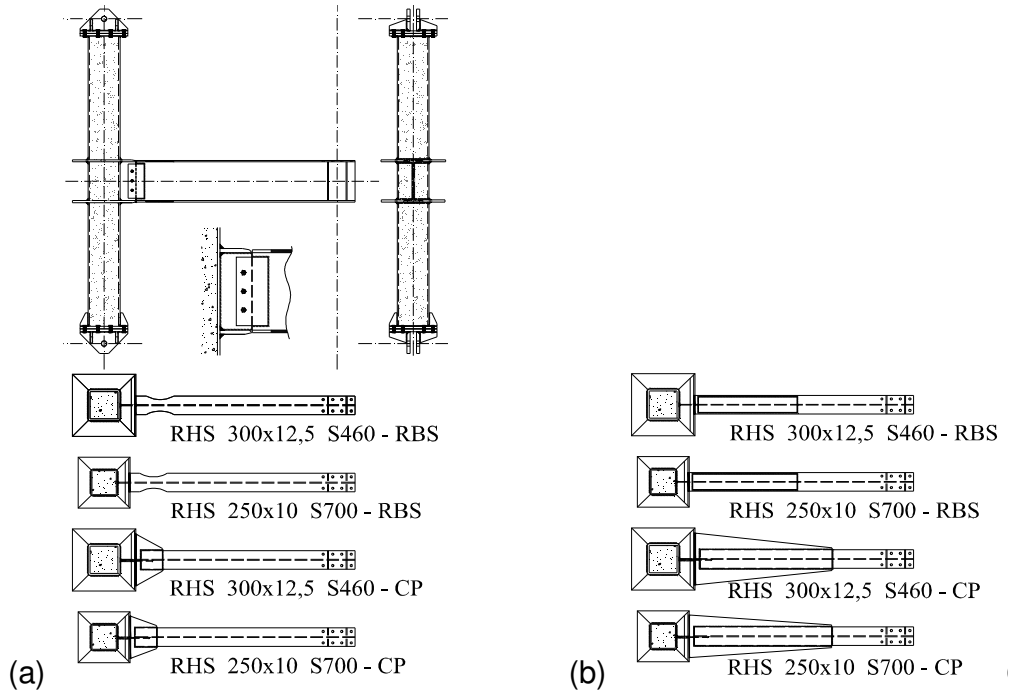

Figure 7. a) Configuration of the designed joint specimens, and b) the reinforced joints

The experimental program to be performed on beam-to-column joints is summarized in Table 1. The variations in the configuration of the beam-to-column joints are given by two joint typologies (reduced beam section and cover-plate), two steel grades for the tubes (S460 and S700) and two failure modes (plasticization in the beam and in the connection zone).

Table 1. Test program on welded beam-to-column joints

Parameter	Variable	No. of variations	No. of specimens
Loading procedure	Monotonic and cyclic	2	16
Joint type	RBS and CP	2	
HSS grade	S460 and S700	2	
Failure mode	Weak beam / Weak connection	2	

The member cross sections and the main components of the four designed joints (see Figure 7a) are summarised in Table 2.

Table 2. Components of the joint specimens displayed in Figure 7a

Joint	Column	Stiffeners	Cover plates	Beam
RBS	RHS 300x12.5 - S460	150x20 - S460	-	IPE 400 - S355
RBS	RHS 250x10 - S700	120x20 - S690	-	IPE 400 - S355
CP	RHS 300x12.5 - S460	150x20 - S460	500x15 - S355	IPE 400 - S355
CP	RHS 250x10 - S700	120x20 - S690	500x15 - S355	IPE 400 - S355

It is intended to extend the experimental program with joint configurations, of larger cross section members, that could not be tested. The cross section of beams and columns (Figure 8), were obtained from frame design performed by Silva *et al.* 2011.

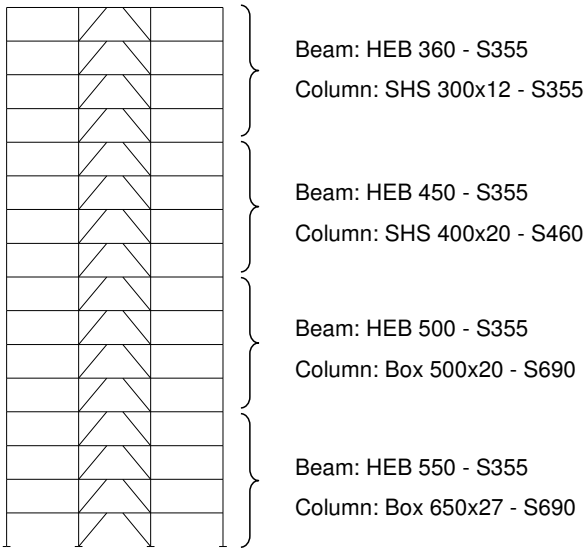

Figure 8. Member cross section of the 16 storey D-EBF designed for soft soil

A number of four additional joints were designed following the same design procedure. The components of the designed joints for the extension of the experimental program are summarised in Table 3.

Table 3. Components of the joints (extension of the experimental program)

Joint	Column	Stiffeners	Cover plates	Beam
RBS	Box 500x20 - S690	200x25 - S690	-	HEA 500 - S355
CP	Box 500x20 - S690	200x30 - S690	700x25 - S355	HEA 500 - S355
RBS*	Box 650x27 - S690	200x30 - S690	-	HEB 550 - S355
CP*	Box 650x27 - S690	250x35 - S690	850x30 - S355	HEB 550 - S355

Note: The cases marked with "*" are presented in Figure 9

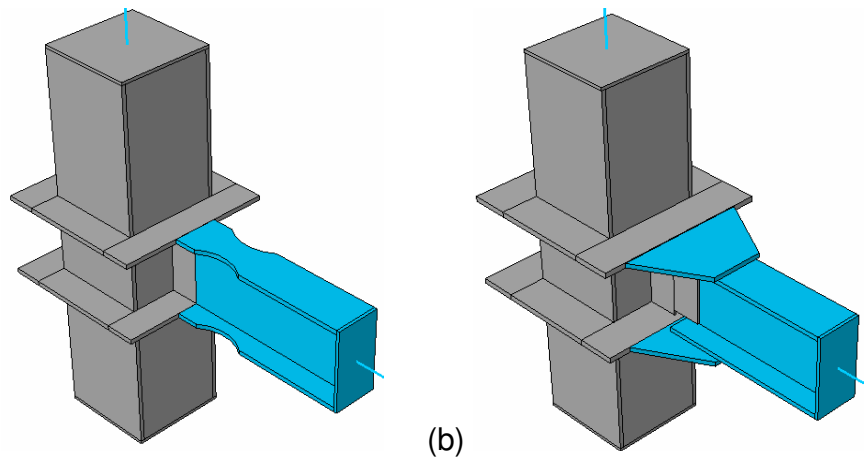

(a) (b)

Figure 9. Extension of the experimental program: a) RBS joint, and b) CP joint

4. NUMERICAL INVESTIGATION

4.1 Numerical testing of the joint specimens

Due to the innovative joint configurations, it was needed to have an accurate prediction for the behaviour of the joints in order to avoid unacceptable failure during the experimental tests. Therefore, numerical simulations have been performed with the finite element modelling software Abaqus (2007). The following parts of the joint configurations were used in the numerical models: concrete filled tube (RHS 300x12.5 S460/RHS 250x10 S700 and concrete C30/37), column stiffeners (plates of S460 and S690 steel grade), beam (IPE 400 S355) and cover plates (S355). All the components of the beam-to-column joint were modelled using solid elements. In order to have in the end a uniform and structured mesh, some components with a complex geometry were partitioned into simple shapes. The engineering stress-strain curves of the steel grades were obtained from the steel producers. The material model was therefore calibrated based on results from tensile tests, converting the engineering stress-strain curves into true stress - true strain curves (Figure 10).

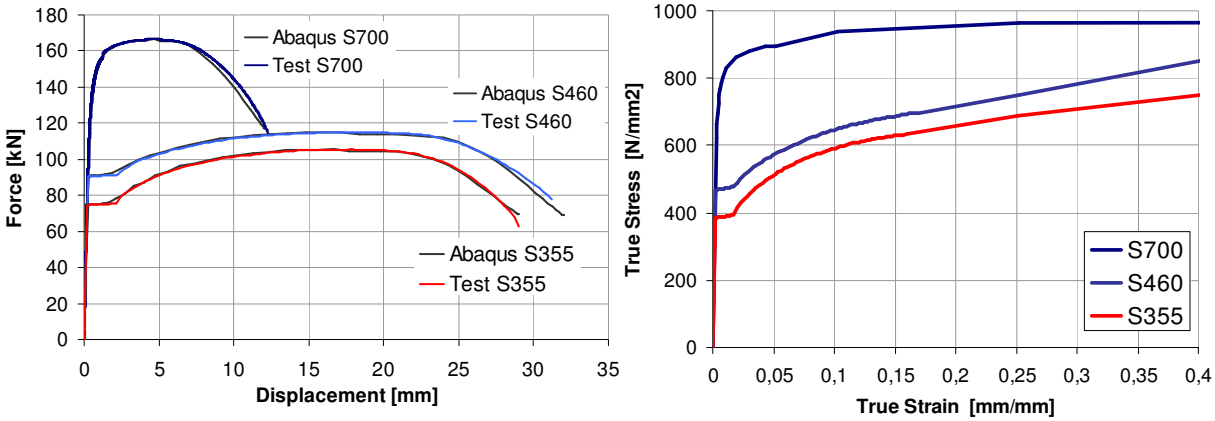

Figure 10. Calibration of the stress-strain curve for the steel grades, a) comparison between test and simulation, and b) the corresponding true stress-strain curves

For the concrete core, the 'concrete damaged plasticity' model was used (Korotkov *et al*., 2004). The different components were assembled together according to each joint configuration. Due to the large amount of contact surfaces between the concrete core and the steel tube, the dynamic explicit type of analysis was used. For the interaction between the steel tube and the concrete core, a normal contact was defined that allows the two parts to separate. The weld between the different parts of the joint configurations was modelled using the tie contact. The load was applied through a displacement control of 250 mm at the tip of the beam and the column was considered as double pinned. The mesh of the elements was done using linear hexahedral elements of type C3D8R.

From the simulations, for each joint configuration, the moment-rotation curve was obtained as well as the stress distribution and plastic strain in the connection and concrete core. According to this, for the RBS and CP joints, yielding was initiated in beam flanges (Figure 11 and Figure 12). Further loading showed an increase of the plastic strain in the upper flange and local buckling of the lower flange and web. For

these configurations, the low deformations of the concrete core confirm that the encased concrete does not crush under the compression at the lower flange level.

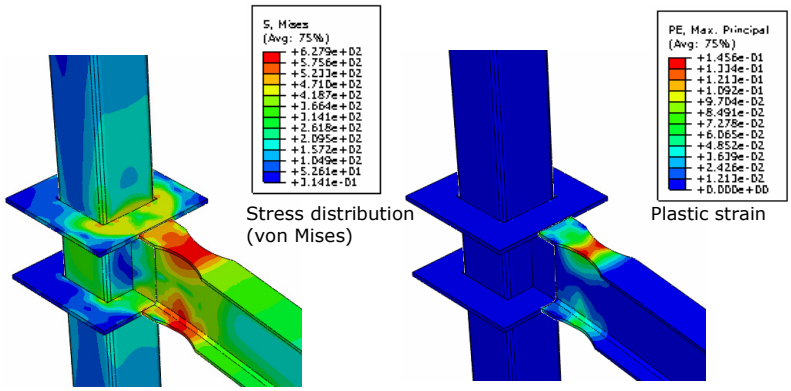

Figure 11. Joint with RBS: von Misses stresses and plastic deformation

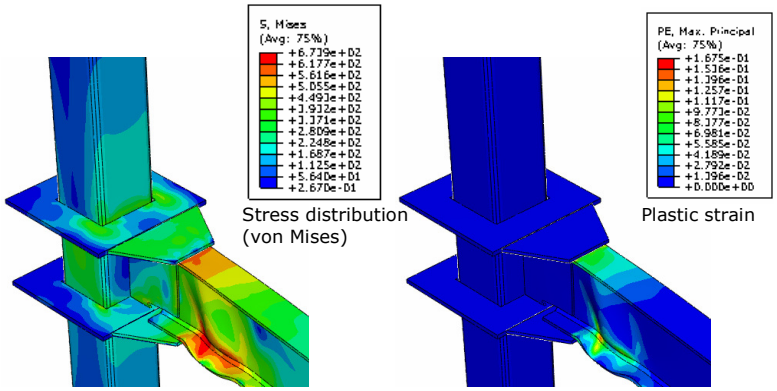

Figure 12. Joint with CP: von Misses stresses and plastic deformation

Figure 13 shows the contribution of the components considered in the design (i.e. beam, column stiffeners and column panel zone) to the overall joint rotation. Low rotation can be observed within the column panel and stiffeners, the main deformations being developed in the beam.

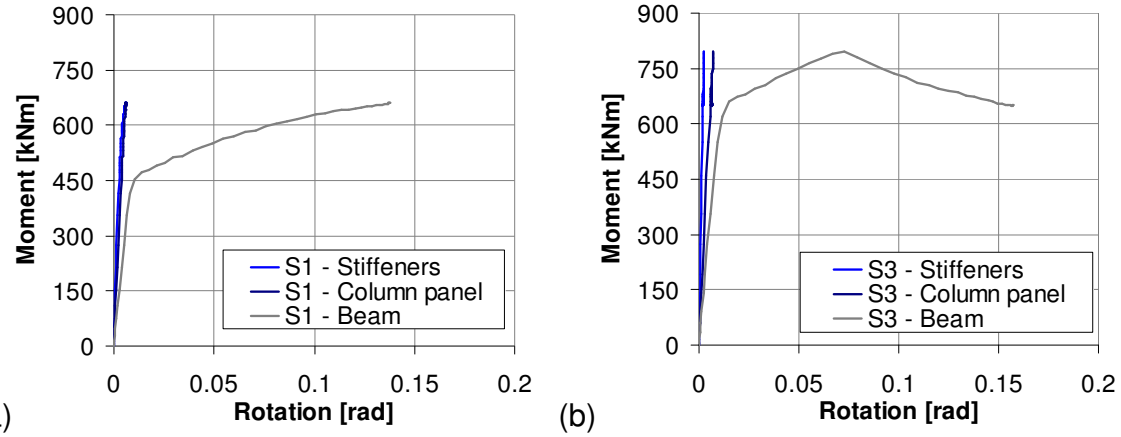

Figure 13. Contribution of components to joint rotation: a) RBS, b) CP

For the joints with strengthened beam, yielding was initiated in the adjacent area of the welded on-site connection (Figure 14), and respectively in the column panel zone (Figure 15). For these configurations, the failure mechanism is described by large plastic deformations in the upper flange connection for the strengthened RBS joint and steel tube and concrete core for the strengthened CP joint.

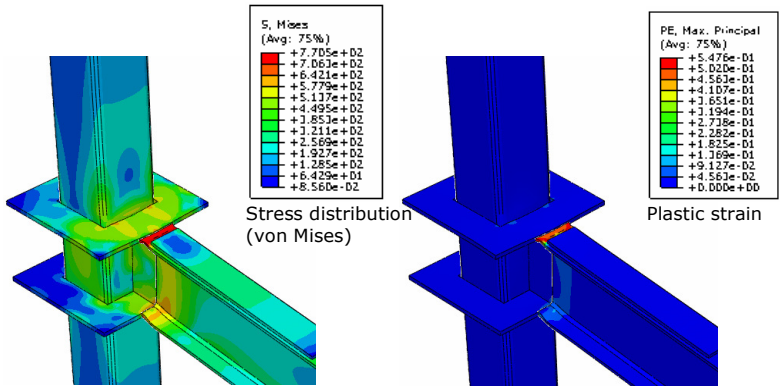

Figure 14. Joint with strengthened flanges: von Misses stresses and plastic deformation

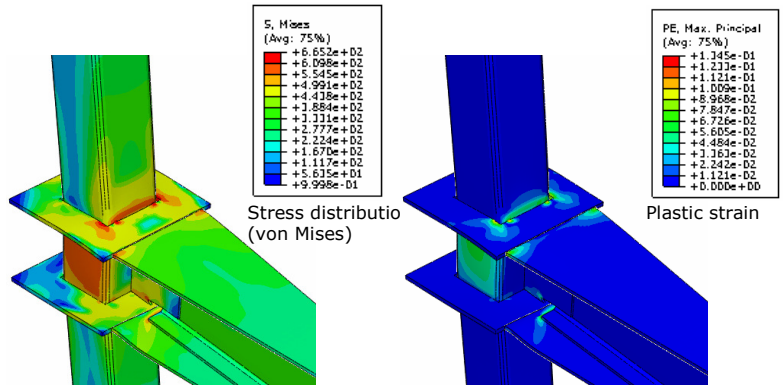

Figure 15. Joint with extended cover-plates: von Misses stresses, plastic deformation

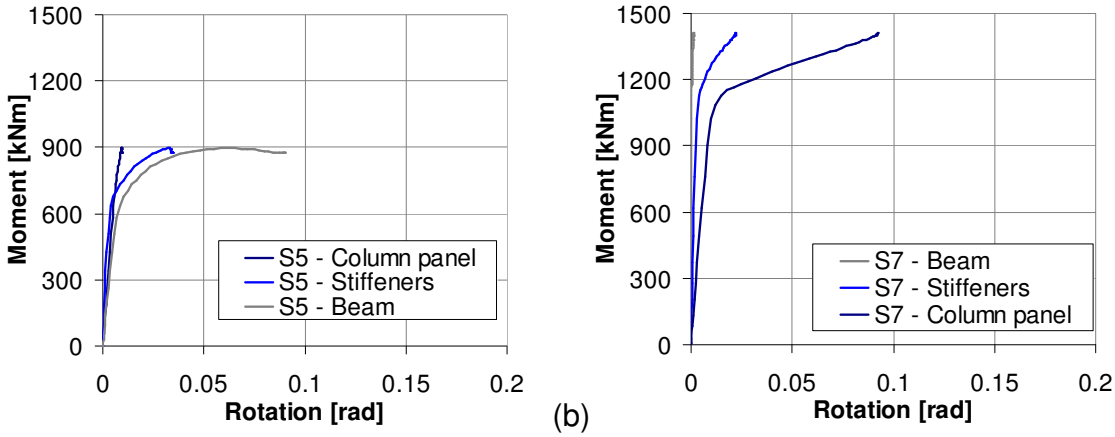

Figure 16. Contribution of components to joint rotation: a) strengthened RBS joint, b) joint with extended cover plates

Figure 16 shows the contribution of the components to the overall joint rotation for the joints with strengthened beam. In the first case, low rotations can be observed within the column panel, the main rotations being developed in the beam near the welded connection and in a lower amount in the stiffeners. In the second case, the rotations in the beam are extremely low, the main rotations being developed in the column panel zone and in a lower amount with the stiffeners.

Considering the overall displacement of 250 mm applied at the tip of the beam, the maximum plastic strain reached a value of 14% in the upper flange of the RBS joints, 16% in the upper flange of the CP joints, 54% in the upper flange of the strengthened RBS joints, and 13% in the steel tube of the strengthened CP joints. Comparing these values with the material model described in Figure 10, it can be observed that in the case of the designed RBS and CP joints the plastic strain is lower than the ultimate tensile strain related to fracture. In contrast, for the case of the joints with strengthened beam, the values of the plastic strain are higher than the expected strain at fracture.

Therefore, these preliminary numerical simulations predict the failure mechanism and confirm the assumptions used for the design of the joints (formation of the plastic hinge in the beam), and check the feasibility of the adopted solution for the testing set-up and instrumentation.

The moment-rotation curves corresponding to the joints with weak beam as failure mode (formation of the plastic hinge in the beam) are shown in Figure 17. It can be observed that the joints with cover plates (CP) have a higher resistance compared to the joints with reduced beam section (RBS). For the same joint typology, the stiffness is higher for the case with larger column cross section (RHS 300x12.5).

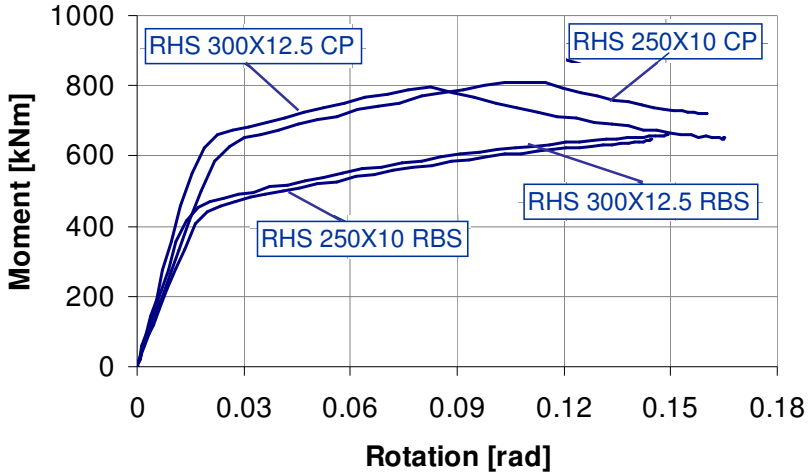

Figure 17. Moment-rotation curves for joints with weak beam as failure mode

4.2 Extension of the experimental program

Numerical simulations were performed also for the joints with larger cross section members. The contribution of the components considered in the design (i.e. beam, column stiffeners and column panel zone) to the joint rotation, are shown in Figure 18a for the RBS joint and in Figure 18b for the CP joint. As in the case of the joints designed for the experimental program, low rotations can be observed within the column panel

zone and stiffeners, the main deformations being developed, for both cases, in the beam. In addition, the stress distribution and plastic strain, shown in Figure 19 and Figure 20, confirm the development of large plastic deformations in the beam.

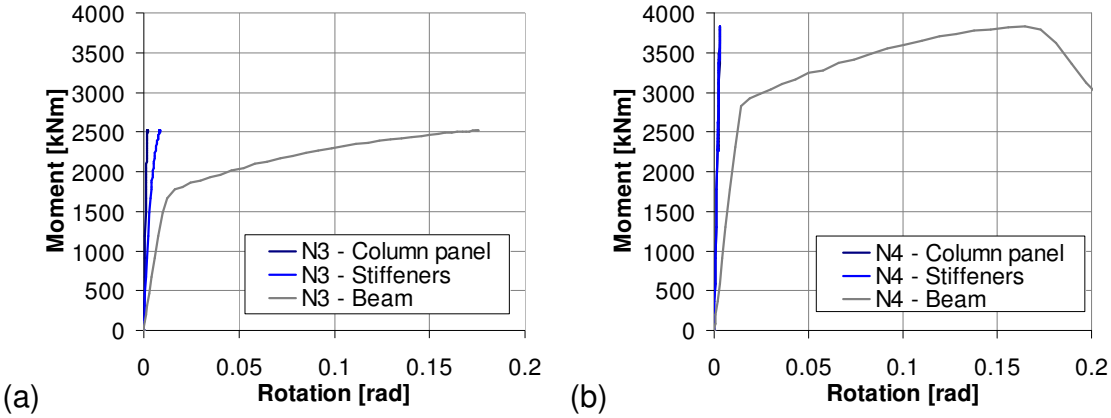

Figure 18. Contribution of components to joint rotation: (a) RBS joint, (b) CP joint

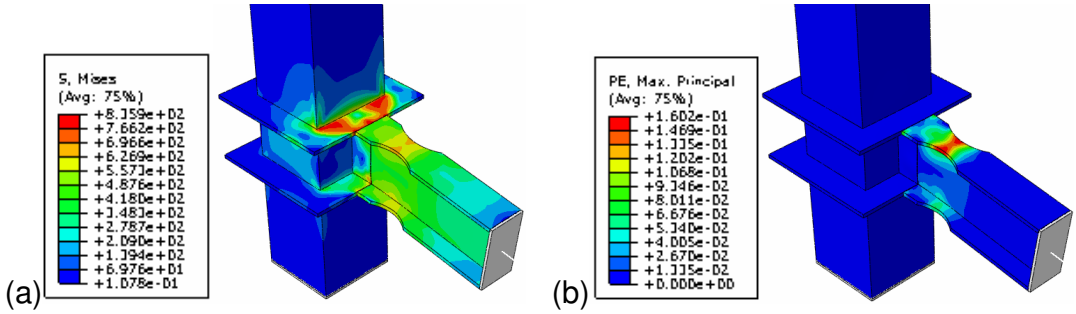

Figure 19. RBS joint: von Misses stresses, plastic deformation

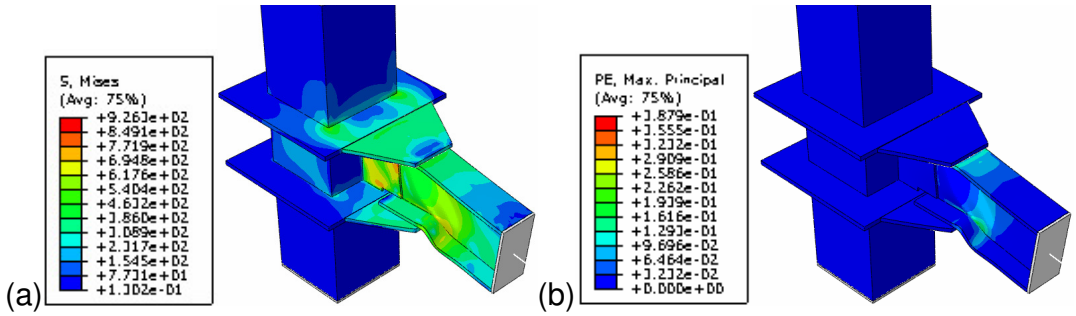

Figure 20. CP joint: von Misses stresses, plastic deformation

In addition, for the joint with cover plates (CP) designed for the experimental program, a numerical analysis was performed with the aim to investigate the influence of the axial force within the column on the behaviour of the joint. The level of axial force introduced in the column was $0.5 \cdot N_{pl,Rd}$. Figure 21 shows the moment-rotation curves corresponding to the joint without axial force in the column and to the compressed column. No significant difference can be observed between the two cases, with the remark that the axial force lead to a very low increase in resistance.

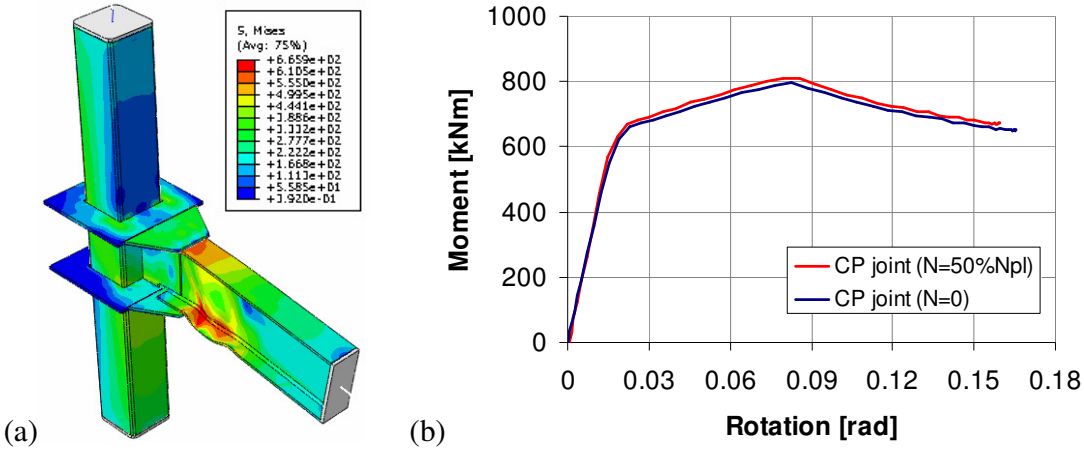

Figure 21. CP joint: a) von Misses stresses, b) moment-rotation curves

5. CONCLUSIONS

The paper makes a short description of the dual-steel concept that is to be investigated through experimental tests on beam-to-column joints. The purpose is to assess the joint characteristics in terms of resistance, stiffness and rotation capacity. Components of each joint connection were identified and designed according to current design codes. The question is if there are components that were not taken into account in the design process. Therefore the experimental tests on joint specimens will help investigate the main components of the joints. The joint typology and the connection details between beams and columns were presented together with the assumptions taken into account in the design process. Additionally, due to the innovative joint configuration, a set of numerical simulations has been performed for the joints designed for the experimental program, as well as for joints with larger cross section members. Based on the results obtained, the numerical simulations prove a good configuration and design of the joints. For the joints where the plastic hinge formed in the beam, the other components (welded on-site connection, stiffeners, column panel) fulfil their job. In contrast, for the joints with strengthened beams, the simulations evidence a weakness of the joint configurations in terms of welded on-site connection and column panel. The axial force in the column was observed to have a low influence on the joint behaviour.

Further research activities will be devoted to the calibration of the numerical models based on joint tests. The joint characteristics obtained experimentally and from the numerical simulations will be applied on the investigated structures with the purpose to assess the seismic performance and robustness of dual-steel frames.

6. ACKNOWLEDGEMENT

The first author was partially supported by the strategic grant POSDRU/88/1.5/S/50783, Project ID50783 (2009), co-financed by the European Social Fund - Investing in People, within the Sectoral Operational Program Human Resources Development 2007-2013.

The present work was supported by the funds of European Project HSS-SERF: "High Strength Steel in Seismic Resistant Building Frames", Grant N0 RFSR-CT-2009-00024.

REFERENCES

Morino S., Tsuda K. Design and construction of concrete-filled steel tube column system in Japan, Earthquake Engineering and Engineering Seismology, Vol. 4, No. 1, 2003, pp. 51–73.

Park J. W., Kang S.M., Yang S. C. Experimental studies of wide flange beam to square concrete-filled tube column joints with stiffening plates around the column, Journal of Structural Engineering © ASCE, Vol. 131, No. 12, 2005, pp. 1866–1876.

Kurobane Y., Packer J. A., Wardenier J., Yeomans N. Design guide for structural hollow section column connections, TÜV Verlag, Köln, 2004.

AISC 358 (2005), Prequalified Connections for Special and Intermediate Steel Moment Frames for Seismic Applications, AISC, American Institute of Steel Construction.

PEER Report 2000/07 (2000), Cover-Plate and Flange-Plate Reinforced Steel Moment-Resisting Connections, Pacific Earthquake Engineering Research Center.

EN1998-1-1 (2004), Eurocode 8, Design of structures for earthquake resistance - Part 1, General rules, seismic actions and rules for buildings, CEN, European Committee for Standardization.

EN1994-1-1 (2004), Eurocode 4, Design of composite steel and concrete structures - Part 1, General rules and rules for buildings, European Committee for Standardization.

Abaqus (2007) Analysis User's Manual I-V. Version 6.7. USA: ABAQUS, Inc., Dassault Systèmes.

Korotkov V., Poprygin D., Ilin K., Ryzhov S. (2004), Determination of dynamic reaction in concrete floors of civil structures of nuclear power plant in accidental drops of heavy objects, ABAQUS Users' Conference, Boston, 25-27 May, 2004, pp. 399-408.

Silva L.S., Rebelo C., Serra M., Tenchini A. (2011), "Selection of structural typologies and design of optimized dual-steel multi-storey frames", Mid Term Report HSS-SERF Project: "High Strength Steel in Seismic Resistant Building Frames", Grant N0 RFSR-CT-2009-00024.

Vulcu C., Stratan A., Dubina D. (2012 – in print), Seismic Performance of EB Frames of Composite CFHS High Strength Steel Columns, *10th International Conference on Advances in Steel Concrete Composite and Hybrid Structures*, Singapore, 2–4 July 2012, (in print).

Vulcu C., Stratan A., Dubina D. (2012 – in print), Seismic performance of dual frames with composite CF-RHS high strength steel columns, *15th World Conference on Earthquake Engineering, Lisbon*, 24–28 September 2012, (in print).